Parameter analysis for a nuclear magnetic resonance gyroscope based on ^{133}Cs–^{129}Xe/^{131}Xe*

Da-Wei Zhang(张大伟), Zheng-Yi Xu(徐正一), Min Zhou(周敏), and Xin-Ye Xu(徐信业)†

State Key Laboratory of Precision Spectroscopy, East China Normal University, Shanghai 200062, *China*

(Received 12 October 2016; revised manuscript received 24 November 2016; published online 20 December 2016)

We theoretically investigate several parameters for the nuclear magnetic resonance gyroscope based on ^{133}Cs–^{129}Xe/^{131}Xe. For a cell containing a mixture of ^{133}Cs at saturated pressure, we investigate the optimal quenching gas (N_2) pressure and the corresponding pump laser intensity to achieve 30% ^{133}Cs polarization at the center of the cell when the static magnetic field B_0 is 5 μT with different ^{129}Xe/^{131}Xe pressure. The effective field produced by spin-exchange polarized ^{129}Xe or ^{131}Xe sensed by ^{133}Cs can also be discussed in different ^{129}Xe/^{131}Xe pressure conditions. Furthermore, the relationship between the detected signal and the probe laser frequency is researched. We obtain the optimum probe laser detuning from the D2 ($6^2S_{1/2} \rightarrow 6^2P_{3/2}$) resonance with different ^{129}Xe/^{131}Xe pressure owing to the pressure broadening.

Keywords: nuclear magnetic resonance, gyroscope, optical pumping, spin-exchange collision, optical rotation

PACS: 32.10.Dk, 34.10.+x, 51.60.+a **DOI:** 10.1088/1674-1056/26/2/023201

1. Introduction

Atomic gyroscopes are high performance devices sensitive to rotation, which have abundant applications, such as for inertial navigation,[1] studying the Earth's rotation and tests of general relativity.[2] Different from cold atomic gyroscopes based on atomic interference, the nuclear magnetic resonance gyroscope (NMRG) utilizes the nuclear magnetic resonance effect to measure the change of the rotational orientation regarding the nuclear spin Larmor precession rate in the static magnetic field as a stable reference.[3] Basically, NMRG has no moving parts and it is insensitive to the acceleration and the vibration of the gyro housing. It has been developed for several decades since the early table-top version was realized in the 1960s.[4] Recently, NMRG has again attracted considerable attention in that it can meet the requirements of both high precision and miniaturization with the advanced development of microelectronic processing techniques.[5]

NMRGs being developed worldwide mainly employ alkali atoms and noble gases, for instance, a mixture of ^{87}Rb, NMR active medium ^{129}Xe /^{131}Xe together with the buffer gas N_2.[6] There are many theoretical or experimental works on studying spin-exchange parameters for alkali-metal-noble-gas pairs,[7,8] absolute alkali-metal polarization,[9] and surface relaxation of laser-polarized noble-gas.[10] However, the rotation sensitivity associated conditions of these NMRGs, especially the ^{133}Cs–^{129}Xe/^{131}Xe type, are lacking elaborated research. In this work, we detail a discussion on parameters for NMRG based on ^{133}Cs–^{129}Xe/^{131}Xe, including the N_2 pressure, the optical pumping laser intensity, the effective field produced by spin-exchange polarized ^{129}Xe/^{131}Xe magnetization vector sensed by ^{133}Cs, and the optimal frequency detuning of the probe laser and so on. This work is to provide theoretical support for the next step of the NMRG experiment based on ^{133}Cs–^{129}Xe/^{131}Xe.

2. Basic principle of NMRG

The basic principle of NMRG is illustrated in Fig. 1. The ^{133}Cs vapor is optically pumped by a circularly-polarized laser beam[11,12] which propagates along the z axis. A static magnetic field B_0 is applied along the z axis. A net electron spin polarization accumulates in ^{133}Cs atoms. It is then transferred to Xe nuclei through spin-exchange collisions, resulting in a macroscopic nuclear spin polarization for Xe. By applying an oscillating magnetic field $B_1 \cos(\omega_a t)$ along the x axis, the Xe spin magnetic moment M tilts from the z axis, and its component along the xy plane M_{xy} will precess about B_0 with an angular frequency $\omega_{Xe} = \gamma B_0$, where ω_a approximately equals to ω_{Xe} and the proportional constant γ is the gyromagnetic ratio of Xe. The ^{133}Cs spins precess about the total magnetic field, which is the sum of B_0 and the Xe spins generated part. Since the alkali-metal atoms are more susceptible to the magnetic field than the noble gas,[13] a linearly-polarized probe laser beam whose frequency is near resonant with the ^{133}Cs optical transition may rotate its polarization of the macroscopic field component along the x axis of the polarized Xe atoms precess about B_0 field, the photoelectric detector accepted laser intensity will periodically vary after the probe laser passes through the linear polarizer. Assuming the gyroscope is rotating about

*Project supported by the National High Technology Research and Development Program of China (Grant No. 2014AA123401), the National Key Basic Research and Development Program of China (Grant Nos. 2016YFA0302103 and 2012CB821302), the National Natural Science Foundation of China (Grant 11134003), and Shanghai Excellent Academic Leaders Program of China (Grant No. 12XD1402400).

†Corresponding author. E-mail: xyxu@phy.ecnu.edu.cn

© 2017 Chinese Physical Society and IOP Publishing Ltd

the z axis at a frequency ω_R, the measured Larmor precession frequency will change from the reference ω_{Xe} to be

$$\omega_M = \omega_{Xe} + \omega_R. \quad (1)$$

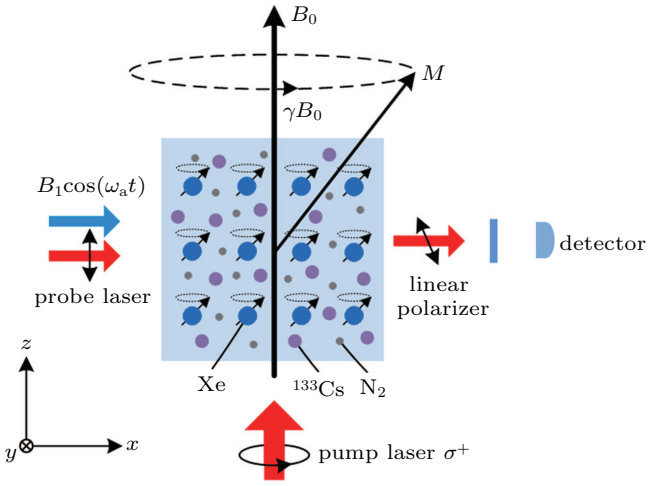


Fig. 1. (color online) Basic principle of NMRG. The circularly σ^+ polarized pump light along the z axis, the linear polarized probe light and oscillating magnetic field along the x axis. The combination of linear polarizer and detector is used to detect the polarization rotation of the probe light.

To determine ω_R, precise knowledge and careful control of B_0 are needed. A two-NMR-isotope method fundamentally uncouples ω_R from B_0, reducing the difficulty in stabilizing B_0. To this end, both ^{129}Xe and ^{131}Xe are contained in the vapor cell which means they have the same ω_R. Since γ of ^{129}Xe and ^{131}Xe have different values and opposite signs, they have their respective precession frequencies[14]

$$\begin{aligned} \omega_1 &= \gamma_{^{129}\mathrm{Xe}} B_0 + \omega_R, \\ \omega_2 &= \gamma_{^{131}\mathrm{Xe}} B_0 - \omega_R, \end{aligned} \quad (2)$$

where $\gamma_{^{129}\mathrm{Xe}}$ and $\gamma_{^{131}\mathrm{Xe}}$ are gyromagnetic ratios of ^{129}Xe and ^{131}Xe. Therefore, ω_R can be deduced by simultaneously monitoring ω_1 and ω_2, where B_0 is seen as a removable common-mode parameter and

$$\omega_R = \frac{\gamma_{^{131}\mathrm{Xe}}\omega_1 - \gamma_{^{129}\mathrm{Xe}}\omega_2}{\gamma_{^{129}\mathrm{Xe}} + \gamma_{^{131}\mathrm{Xe}}}.$$

3. Calculation and results

In our proposed experiment, a cubic glass cell with side length $L = 2.5$ cm is heated to near 110 °C to obtain optimal balance between the relatively long lifetime and the high signal to noise ratio of ^{133}Cs,[15] containing ^{133}Cs at the saturated vapor pressure and gas mixture ^{129}Xe/^{131}Xe are 4×10^3 Pa/1.6×10^4 Pa (mixture I), 6.67×10^3 Pa/2.67×10^4 Pa (mixture II), 1.07×10^4 Pa/4.27×10^4 Pa (mixture III).[16] Next, we take mixture II as an example to discuss the relationship between pump laser intensity and N_2 pressure. In the presence of a static magnetic field B_0 applied along the z axis, a circularly σ^+ polarized pumping-light[17] resonant with the ^{133}Cs D1[18] ($6^2S_{1/2} \rightarrow 6^2P_{1/2}$) line is applied to optically pump the alkali atoms to the Zeeman substates $^2S_{1/2}$ ($F = 4$, $m_F = 4$) ground state. The position-dependent pump rate $R_p(z)$ of ^{133}Cs in the cell is given by[19]

$$\frac{dR_p}{dz} = -n_{Cs}\sigma(\nu_0)(1 - P^e)R_p, \quad (3)$$

where n_{Cs} denotes the cesium atomic density, the normalized polarization P^e is the ^{133}Cs polarization and defined as $R_p/(R_p + R_{tot})$ with R_{tot} being the total spin-relaxation rate, here we consider R_{tot} as a fixed value, and $\sigma(\nu_0)$ is the photon absorption cross-section at the resonance frequency ν_0. For the D1 line of ^{133}Cs, the linewidths broadened by the ^{129}Xe/^{131}Xe and N_2 (for 2.67×10^4 Pa) pressures are 6 GHz and 6.8 GHz[20] respectively for mixture II. For comparison, the natural linewidth is 4.6 MHz and the Doppler broadening linewidth is 427 MHz. Thus Γ_{D1} is dominated by the pressure broadening, $\sigma(\nu_0)$ approximately equals to $2cr_e f_{D1}/\Gamma_{D1}$, where r_e is the classical electron radius, c is the speed of light, f_{D1} is the D1 transition oscillator strength, and Γ_{D1} is the transition linewidth.

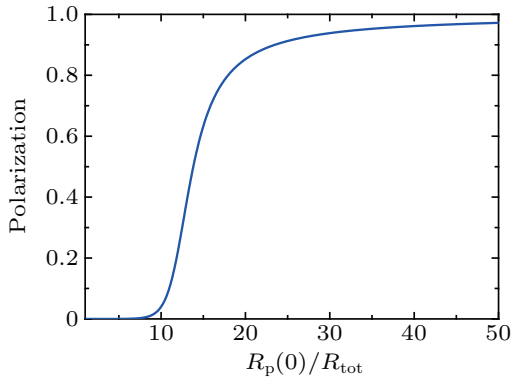


Fig. 2. (color online) The ^{133}Cs polarization as a function of different $R_p(0)/R_{tot}$ conditions at the center of the cell.

The principal value of the Lambert W-function (the inverse of the function $f(W) = We^W$) describes the solution of Eq. (3), which is given by

$$R_p(z) = R_{tot} W\left\{\frac{R_p(0)}{R_{tot}} \exp\left[-zn_{Cs}\sigma(\nu_0) + \frac{R_p(0)}{R_{tot}}\right]\right\}, \quad (4)$$

where $R_p(0)$ is the pump rate at $z = 0$, i.e., at the front of the cell. The ^{133}Cs polarization $P_e(z) = R_p(z)/(R_p(z) + R_{tot})$, we perform the ^{133}Cs polarization as a function of different $R_p(0)/R_{tot}$ conditions at the center of the cell, as shown in Fig. 2. When the pump rate is comparable to the total spin-relation rate, the polarization is small. When the pump rate is much higher than the total spin-relation rate, the polarization rapidly increases first and then slowly increases. In NMRG, obtaining high polarization of ^{133}Cs is difficult and the obtainable highest ^{133}Cs polarization is about 20% at present.[15] Here we will discuss the relevant parameter to achieve 30%

^{133}Cs polarization. In order to obtain 30% ^{133}Cs polarization at the cell center, from Fig. 2 we know $R_{\rm p}(0)/R_{\rm tot}$ should be controlled around 12.48 by adjusting the pump laser intensity.

A phenomenon known as radiation trapping may degrade the polarization of the alkali vapor. Radiation trapping happens when the unpolarized photons scattered by excited ^{133}Cs atoms through spontaneous emission are reabsorbed by other adjacent atoms. In our case, a quenching gas N_2[11,12] is added to it to create a pathway for the atoms to decay to the ground state without emitting photons at all. The fraction of atoms that reach the ground state by emitting a photon rather than quenching is given by $Q = 1/\left(1+p_{N_2}/p'_Q\right)$, where p_{N_2} is the N_2 pressure, and p'_Q is a characteristic pressure. For the D1 line of ^{133}Cs at 110 °C, p'_Q is 473 Pa.[22] The spin-relaxation rate due to radiation trapping is $R_{\rm rt} = K(N-1)QR_{\rm p}(1-P^{\rm e})$, where K describes the degree of depolarization caused by reabsorbing a photon, N is the average number of times that a photon is emitted before it leaves the vapor cell. Note that $R_{\rm rt}$ is proportion to $R_{\rm p}$, so the radiation trapping effect is also location-dependent. In the presence of the quenching gas, the obtainable ^{133}Cs polarization at the cell center is

$$P_{\rm c}^{\rm e} = \frac{1}{1+R_{\rm rel}/R_{\rm p_c}+K(N-1)Q(1-P_{\rm c}^{\rm e})}, \tag{5}$$

where $R_{\rm p_c}$ is the pump rate at the center of the cell and $R_{\rm rel}$ is the relaxation rate due to effects other than radiation trapping. K is always below 1 due to uncompleted depolarization. In theory, a reasonable value of K is 0.06 according to Ref. [22] and N is calculated about 75 for mixture II when N_2 pressure is 2.67×10^4 Pa.[23] In fact, when p_{N_2} is set to be dozens of Torr (1 Torr = 1.33322×10^2 Pa), $R_{\rm rel}$ will be much larger than $R_{\rm rt_c}$, which means the polarization is not mainly limited by the radiation trapping.

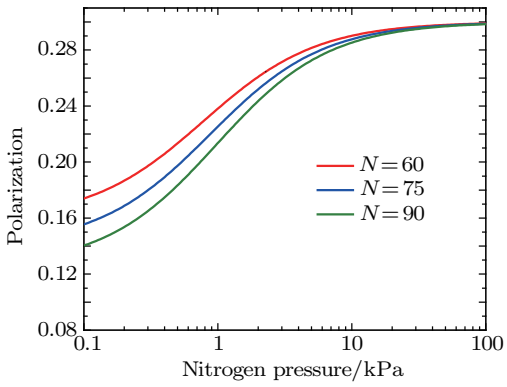


Fig. 3. (color online) The ^{133}Cs polarization at the center of the cell as a function of the N_2 pressure with different N.

Figure 3 shows the ^{133}Cs polarization at the center of the cell as a function of N_2 pressure with N around 75 when assuming $R_{\rm rel}/R_{\rm p_c} \approx R_{\rm tot}/R_{\rm p_c} = 2.333$. The figure indicates that the polarization will keep growing until saturation as the N_2 pressure increases. It shows that at the cell center ^{133}Cs polarizability is about 29.5% (less than 30%) when $p_{N_2} = 2.67\times10^4$ Pa, which indicates that the radiation trapping cannot be ignored. Meanwhile, the similar tendency of three lines suggests that the polarization is insensitive to N when $p_{N_2} = 2.67\times10^4$ Pa, which means that the ^{133}Cs polarization is stable when various errors are taken into consideration in this regime.

Apart from the radiation trapping, several other effects contribute to the total relaxation rate, which is given by

$$R_{\rm tot} = R_{\rm rt} + R_{\rm se}^{\rm ee} + R_{\rm sd}^{\rm collisions} + R_{\rm se}^{\rm en} + R_{\rm D} + R_{\rm m}, \tag{6}$$

where $R_{\rm se}^{\rm ee}$ is the Cs–Cs spin-exchange collisional term, $R_{\rm sd}^{\rm collisions}$ is the spin-destruction collisional term, $R_{\rm se}^{\rm en}$ is the Cs–Xe spin-exchange collisional term, $R_{\rm D}$ is the term of diffusion to the walls, and $R_{\rm m}$ is the probe laser pumping term.

As aforementioned, the spin-relaxation rate due to radiation trapping is related to $P^{\rm e}$, which is nonuniform throughout the cell, here we assume $R_{\rm rt} \approx K(N-1)Q\bar{R}_{\rm p}(1-\bar{P}^{\rm e})$, $\bar{R}_{\rm p}$ and $\bar{P}^{\rm e}$ are the mean pump rate and mean polarizability from $z=0$ to the cell center respectively, thus $R_{\rm rt} \approx 0.0078R_{\rm p}(0)$. In actual experiments, the probe laser frequency is tuned far from resonance and the laser power is usually relatively low. Therefore, the probe laser pumping term $R_{\rm m}$ can also be ignored. Spin-exchange collisions between alkali metal atoms are very fast and $R_{\rm se}^{\rm ee}$ can be estimated as[24]

$$R_{\rm se}^{\rm ee} = \left(\frac{\gamma_{\rm e}B_0}{Q(\bar{P}^{\rm e})}\right)^2 T_{\rm se}\frac{Q(\bar{P}^{\rm e})^2-(2I+1)^2}{2}, \tag{7}$$

where $Q(\bar{P}^{\rm e})$ is the slowing down factor, $1/T_{\rm se}$ denotes the spin-exchange rate, $\gamma_{\rm e}$ is the gyromagnetic ratio of ^{133}Cs, and I is ^{133}Cs nuclear spin. In the magnetic field $B_0 = 5$ μT, $R_{\rm se}^{\rm ee}$ is calculated to be 1.27×10^5 s^{-1}. The relaxation term of spin-destruction collisions between ^{133}Cs and other elements in the cell is[7]

$$\begin{aligned} R_{\rm sd}^{\rm collisions} = {} & \sigma_{^{129}{\rm Xe}}^{\rm sd}\bar{v}_{^{129}{\rm Xe}}n_{^{129}{\rm Xe}} + \sigma_{^{131}{\rm Xe}}^{\rm sd}\bar{v}_{^{131}{\rm Xe}}n_{^{131}{\rm Xe}} \\ & + \sigma_{\rm N_2}^{\rm sd}\bar{v}_{\rm N_2}n_{\rm N_2} + \sigma_{\rm Cs}^{\rm sd}\bar{v}_{\rm Cs}n_{\rm Cs}, \end{aligned} \tag{8}$$

where $\sigma_{^{129}{\rm Xe}}^{\rm sd}$, $\sigma_{^{131}{\rm Xe}}^{\rm sd}$, $\sigma_{\rm N_2}^{\rm sd}$, and $\sigma_{\rm Cs}^{\rm sd}$ are spin-destruction cross-sections of Cs–^{129}Xe, Cs–^{131}Xe, Cs–N_2, and Cs–Cs collisions respectively, and $\bar{v}$ represents the mean velocity. The relaxation rate due to spin-exchange collisions between ^{133}Cs atoms and the NMR medium Xe is

$$R_{\rm se}^{\rm en} = \sigma_{^{129}{\rm Xe}}^{\rm en}\bar{v}_{^{129}{\rm Xe}}n_{^{129}{\rm Xe}} + \sigma_{^{131}{\rm Xe}}^{\rm en}\bar{v}_{^{131}{\rm Xe}}n_{^{131}{\rm Xe}}, \tag{9}$$

where $\sigma_{^{129}{\rm Xe}}^{\rm en}$, $\sigma_{^{131}{\rm Xe}}^{\rm en}$ are spin-exchange cross-sections of Cs–^{129}Xe, Cs–^{131}Xe. Here we approximate $\sigma_{^{131}{\rm Xe}}^{\rm sd} = \sigma_{^{129}{\rm Xe}}^{\rm sd}$ and $\sigma_{^{131}{\rm Xe}}^{\rm en} = \sigma_{^{129}{\rm Xe}}^{\rm en}$ to calculate the relaxation rates in Eq. (8) and Eq. (9). When an alkali atom encounters the glass surface of the cell wall, it will experience the large local electric and magnetic fields produced by ions and molecules within the glass.

The polarized spins undergo a depolarization process with a rate[22–25]

$$R_{\rm D} = \frac{1}{3}\chi \bar{v}_{\rm Cs}\left(\frac{\pi}{L/2}\right)^2, \tag{10}$$

where χ is a diffusion constant. Equation (10) may be written in terms of the total pressure $P_{\rm tot}$ as $R_{\rm D} = 13142/P_{\rm tot}$. For $P_{\rm tot} = 6\times10^4$ Pa, $R_{\rm D} \approx 0$. The relaxation rate $R_{\rm rel}$ is 1.68×10^5 s^{-1}. Together with the result of $R_{\rm p}(0)/(R_{\rm rel}+R_{\rm rt}) = 12.48$, $R_{\rm p}(0)$ turns out to be 2.32×10^6 s^{-1}.

Now we come to estimate the pumping laser intensity. According to the pumping scheme shown in Fig. 1, the optical pumping rate can be expressed as

$$R_{\rm P} = \frac{2Pcr_{\rm e}f_{\rm D_1}}{h\nu_0 A\Gamma_{\rm D1}}, \tag{11}$$

where P is the pump laser power, h is the Planck constant, and A is the pump laser facula area, $\Gamma_{\rm D1}$ is the broadening linewidth of the D1 line, and $f_{\rm D1}$ is the D1 transition oscillator strength of ^{133}Cs. To meet the requirement of $R_{\rm p}(0)$=2.32×10^6 s^{-1}, the pumping laser intensity P/A is calculated to be 1171 mW/cm^2. In this way, we discuss the pump laser intensity of the three kinds of gas mixture with different N_2 pressures to achieve 30% ^{133}Cs polarization at the center of the cell, which is shown in Fig. 4. The pump intensity drops sharply at first then slowly rises. The minimum intensity of mixture I, mixture II and mixture III are 1020 mW/cm^2, 1169 mW/cm^2, and 1371 mW/cm^2 when the N_2 pressure is about 3×10^4 Pa, higher ^{129}Xe/^{131}Xe pressure corresponding to higher minimum pump laser intensity to achieve the same ^{133}Cs polarization. At present we have developed a Distributed Bragg Reflector (DBR) diode-laser[26] at 895 nm. The laser optical fiber coupling power output exceeds 60 mW. For this purpose, the laser $1/e^2$ beam diameter could be expanded to 3.87 mm, 3.62 mm, and 3.34 mm for mixture I, mixture II, and mixture III respectively.

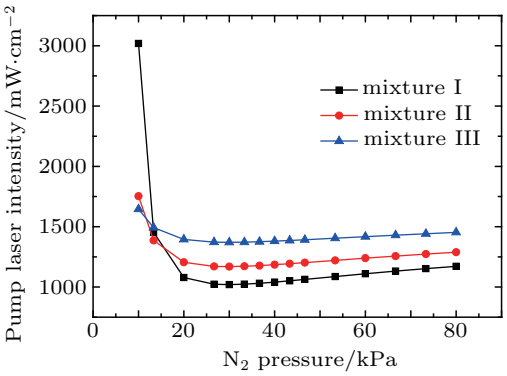


Fig. 4. (color online) The pump laser intensity of the three kinds of gas mixture as a function of the N_2 pressure. The result is obtained to achieve 30% ^{133}Cs polarization at the center of the cell.

The net polarization of ^{133}Cs atoms is transferred to ^{129}Xe/^{131}Xe atoms through spin-exchange collisions. To obtain the same macroscopic nuclear magnetic moment, the pressure ratio of ^{129}Xe and ^{131}Xe has been set to 1:4[16] throughout our discussions. The polarization of ^{129}Xe can be estimated as

$$P_{^{129}\rm Xe} = P^{\rm e}n_{\rm Cs}R^{\rm en}_{{\rm se}^{129}\rm Xe}/(n_{\rm Cs}R^{\rm en}_{{\rm se}^{129}\rm Xe} + n_{\rm n}/T_1^{\rm n}), \tag{12}$$

where $R^{\rm en}_{{\rm se}^{129}\rm Xe}$ is the ^{133}Cs–^{129}Xe spin-exchange rate, $n_{\rm n}$ is the ^{129}Xe atomic density, and $T_1^{\rm n}$ is the longitudinal spin relaxation time of ^{129}Xe. $T_1^{\rm n}$ can reach about 20 s even without anti-relaxation coating of the cell wall. By applying a specified oscillating magnetic field perpendicular to B_0, the Xe spins will precess about the B_0 direction, generating a precessing macroscopic magnetic field. The magnitude of the macroscopic magnetic field has an important influence on the detected signal and can be expressed as[27]

$$B_{^{129}\rm Xe} = \frac{2}{3}\mu_0\kappa_0\mu_{^{129}\rm Xe}P_{^{129}\rm Xe}n_{\rm n}, \tag{13}$$

where μ_0 is the vacuum permeability, κ_0 is the enhancement factor of the Cs–^{129}Xe interaction, and $\mu_{^{129}\rm Xe}$ is the ^{129}Xe nuclear magnetic moment. The effective field sensed by ^{133}Cs due to polarized ^{129}Xe or ^{131}Xe magnetization is about 181 nT, 302 nT, and 484 nT for mixture I, mixture II, and mixture III respectively.

Since alkali metal atoms are very sensitive to the magnetic field, the Larmor precession frequencies of ^{129}Xe and ^{131}Xe can be measured by using the polarized ^{133}Cs atoms. An off-resonance linearly-polarized probe laser beam will rotate its polarization when it interacts with the polarized ^{133}Cs, which is known as the Faraday rotation effect. As shown in Fig. 1, the probe beam propagates along the x-axis, which is orthogonal to the pump beam. The detected rotation signal is given by[22]

$$S = \frac{\pi}{4}Lr_{\rm e}cf_{\rm D2}n_{\rm Cs}P^{\rm e}I_0\,{\rm e}^{-n_{\rm Cs}\sigma(\nu)L} \times \sum_{F\to F'}A_{FF'}\frac{\nu-\nu_{FF'}}{(\nu-\nu_{FF'})^2+(\Gamma_{\rm D2}/2)^2}, \tag{14}$$

where $f_{\rm D2}$ is the D2 transition oscillator strength of ^{133}Cs, $\nu_{FF'}$ and ν are the ^{133}Cs D2 hyperfine transitions resonance frequency and the probe laser frequency respectively, $\Gamma_{\rm D2}$ is the broadening linewidth of the D2 line, $A_{FF'}$ is the relative strength of the hyperfine transition $F\to F'$, and I_0 is the probe laser intensity. From Eq. (14), we know that the probe laser intensity is proportional to the detect signal and it does not affect the optimal probe laser frequency detuning. The photon absorption cross section of cesium is written by

$$\sigma(\nu) = r_{\rm e}cf_{\rm D2}\sum_{F\to F'}A_{FF'}\frac{\Gamma_{\rm D2}/2}{(\nu-\nu_{FF'})^2+(\Gamma_{\rm D2}/2)^2}, \tag{15}$$

which contains the overall contributions of the D2 line hyperfine transitions. The dependences of the optical rotation signal on the probe laser detuning of the three types of ^{129}Xe/^{131}Xe

mixtures are shown in Fig. 5. The signals are somewhat like the dispersion shaped type. The differences are that there are little optical rotations around the resonant frequency. The maximum rotation signals are obtained when the probe laser frequencies are 92 GHz, 106 GHz, and 124 GHz for mixture I, mixture II, and mixture III detuning from the D2 resonance.

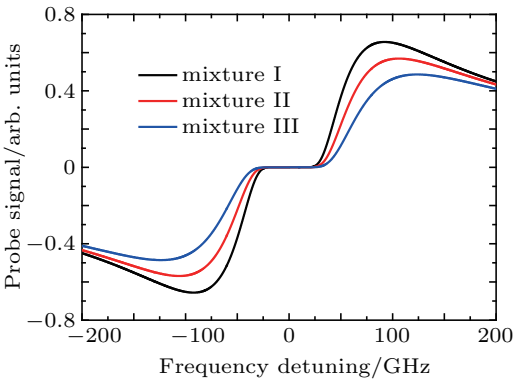


Fig. 5. (color online) The dependence of optical rotation signal on the probe laser detuning of the three kinds of gas mixture.

4. Conclusions

In summary, we have theoretically investigated the interaction between light and atoms, and the interaction between atoms and atoms of the NMRG based on ^{133}Cs–^{129}Xe/^{131}Xe. We discussed the relationship between quenching gas (N_2) pressure and the corresponding optimal pump laser intensity in different ^{129}Xe/^{131}Xe pressure under given parameter conditions. Meanwhile, we estimated the polarized noble gas macroscopic magnetic field, the higher polarized magnetic field corresponding to the higher pump laser intensity. We also studied the influence of probe laser frequency detuning on the probe signal. The theoretical results in this paper will provide guidance for our subsequent experiments of NMRG based on ^{133}Cs–^{129}Xe/^{131}Xe.

References

[1] Fang J C and Qin J 2012 *Sensors* **12** 6331
[2] Stedman G E 1997 *Rep. Prog. Phys.* **60** 615
[3] Donley E A 2010 *Proceedings of the* 2010 *IEEE Sensors Conference*, November 1–4, 2010, Kona, HI, USA, p. 17
[4] Simpson J H, Fraser J T and Greenwood I A 1963 *IEEE Trans. Aerosp.* **1** 1107
[5] Eklund E J, Shkel A M, Knappe S, Donley E and Kitching J 2008 *Sens. Actuators A: Phys.* **143** 175
[6] Meyer D and Larsen M 2014 *Gyroscopy and Navigation* **5** 75
[7] Walker T G 1989 *Phys. Rev. A* **40** 4959
[8] Ghosh R K and Romalis M V 2010 *Phys. Rev. A* **81** 043415
[9] Appelt S, Unlü T, Zilles K, Shah N J, Lang S B and Halling H 1999 *Appl. Phys. Lett.* **75** 427
[10] Driehuys B, Cates G D and Happer W 1995 *Phys. Rev. Lett.* **74** 4943
[11] Walker T G and Happer W 1997 *Rev. Mod. Phys.* **69** 629
[12] Liu G B, Sun X P, Gu S H, Feng J W and Zhou X 2012 *Physics* **41** 803 (in Chinese)
[13] Budker D, Kimball D F, Rochester S M, Yashchuk V V and Zolotorev M 2000 *Phys. Rev. A* **62** 043403
[14] Grover B C, Oaks T, Kanegsberg E, Palisades P, Mark J G, Pasadena, Meyer R L and Park C (U.S. Patent) 4 157 495 [1979-10-14]
[15] Mirijanian J J 2012 "Techniques to Characterize Vapor Cell Performance for A Nuclear-Magnetic-Resonance Gyroscope", Ph. D. Dissertation (California: California Polytechnic State University, USA)
[16] Kwon T M and Oaks T (U.S. Patent) 4 461 996 [1984-08-06]
[17] Gan J H, Li Y M, Chen X Z and Liu H F 1996 *Chin. Phys. Lett.* **13** 821
[18] Zhang J H, Zeng X J, Li Q M, Huang Q and Sun W M 2013 *Chin. Phys. B* **22** 053202
[19] Kornack T W 2005 "A Test of CPT and Lorentz Symmetry Using a K^3 He Co-magnetometer", Ph. D. Dissertation (Princeton: Princeton University, USA)
[20] Bernabeu E and Alvarez J M 1980 *Phys. Rev. A* **22** 2690
[21] Franz F A 1968 *Phys. Lett. A* **27** 457
[22] Seltzer S J 2008 "Developments in Alkali-Metal Atomic Magnetometry", Ph. D. Dissertation (Princeton: Princeton University, USA)
[23] Rosenberry M A, Reyes J P, Tupa D and Gay T J 2007 *Phys. Rev. A* **75** 023401
[24] Allred J C, Lyman R N, Kornack T W and Romalis M V 2002 *Phys. Rev. Lett.* **89** 130801
[25] Franzen W 1959 *Phys. Rev.* **115** 850
[26] Chen C, Zhao L J, Qiu J F, Liu Y, Wang W and Lou C Y 2012 *Chin. Phys.B* **21** 094208
[27] Martínez R J, Kennedy D J, Rosenbluh M, Donley E A, Knappe S, Seltzer S J, Ring H L, Bajaj V S and Kitching J 2014 *Nature Commun.* **5** 3908